Journal of Alloys and Compounds 577 (2013) 6–10

Contents lists available at SciVerse ScienceDirect

Journal of Alloys and Compounds

journal homepage: www.elsevier.com/locate/jalcom

In situ synchrotron X-ray diffraction study on the improved dehydrogenation performance of $NaAlH_4$–$Mg(AlH_4)_2$ mixture

Cheng-Hsien Yang [a], Tzu-Teng Chen [a], Wen-Ta Tsai [a,b,*], Bernard Haochih Liu [a]

[a] *Department of Materials Science and Engineering, National Cheng Kung University, Tainan 701, Taiwan*
[b] *Research Center for Energy Technology and Strategy, National Cheng Kung University, Tainan, Taiwan*

ARTICLE INFO

Article history:
Received 23 February 2013
Received in revised form 23 April 2013
Accepted 23 April 2013
Available online 2 May 2013

Keywords:
Complex metal hydrides
$NaMgH_3$
Metathesis
Dehydrogenation reaction
In situ synchrotron X-ray diffraction

ABSTRACT

The dehydrogenation performance and mechanism of the synthesized $NaAlH_4$–$Mg(AlH_4)_2$ powders were investigated by performing thermogravimetric analysis and *in situ* synchrotron X-ray diffraction analysis. $NaAlH_4$ not only facilitates the first step dehydrogenation of $Mg(AlH_4)_2$ in lowering its initial dehydrogenation temperature but also increases the total amount of H_2 released. Besides, MgH_2 and/or Al phases, the products of the first step dehydrogenation reaction, play a catalytic role in lowering the initial dehydrogenation temperature of $NaAlH_4$. The synthesized $NaAlH_4$–$Mg(AlH_4)_2$ mixture has an initial dehydrogenation temperature as low as 120 °C, and is able to release 5.35 wt% H_2 below 350 °C. The self-catalytic dehydrogenation behavior of the $NaAlH_4$–$Mg(AlH_4)_2$ mixture was elaborated in this work with the aid of *in situ* synchrotron XRD.

1. Introduction

To date there is still no large-scale and reliable hydrogen storage method which can operate under moderate pressure and temperature for vehicles powered by fuel cells. Magnesium aluminum hydride, $Mg(AlH_4)_2$, is a promising solid-state hydrogen storage material due to its relatively low dehydrogenation temperature and high theoretical gravimetric hydrogen density of 9.3 wt% [1–3]. As compared to other metal aluminum hydrides, such as $NaAlH_4$ and $LiAlH_4$, the weaker bond energy of $Mg(AlH_4)_2$ can be attributed to the higher electronegativity of Mg, which causes hydride to decompose and release hydrogen at lower temperature [4].

Since the first synthesis of $Mg(AlH_4)_2$ by Wiberg and Bauer [5], this compound has also been produced using cations metathesis by $NaAlH_4$ and $MgCl_2$ via a wet-chemical method [6–8] or a mechano-chemical activation synthesis [9–13]. However, further improvements on the de-/re-hydrogenation properties of the synthesized $Mg(AlH_4)_2$ are necessary for more practical applications. In view of the approaches applied for complex metal hydrides, both the use of catalysts [14–16] and the nano-confinement of hydrides by a nanoporous scaffold [17–23] have been proposed to effectively improve the hydrogen storage performance of $Mg(AlH_4)_2$.

The concept of destabilization [24–26] has also been applied to modify the dehydrogenation reaction by forming alternative species, leading to the changes in the reaction pathways and a decrease in reaction enthalpy. Vajo et al. [27] demonstrated the beneficial effects of silicon on destabilizing LiH and MgH_2 by forming silicide upon thermal dehydrogenation. This work led to a number of studies which examined thermodynamic destabilization, with a focus on mixed hydrides systems, such as $LiBH_4$–MgH_2 [28–33], $LiAlH_4$–MgH_2 [34–38], and $NaAlH_4$–MgH_2 [38,39].

Ismail et al. [39] revealed the modified dehydrogenation steps and improved the dehydrogenation performance of a mixed $NaAlH_4$–MgH_2 system as compared to that of as-milled $NaAlH_4$ or MgH_2 alone. The synergistic effects of the $NaAlH_4$–$Mg(AlH_4)_2$ system are of particular interest because it has similar constituents to the mixed hydrides mentioned above. From another point of view, the feasibility of $NaAlH_4$–$Mg(AlH_4)_2$ mixture with the combined advantages consist of high H_2 capacity of $NaAlH_4$ (5.5 wt% H_2 below 400 °C) and low dehydrogenation temperature of $Mg(AlH_4)_2$ (beginning at about 170 °C) is worth investigating. Srivastava et al. [40] mechano-chemically synthesized a $NaAlH_4$–$Mg(AlH_4)_2$ mixture, and concluded that the dehydrogenation properties of $NaAlH_4$ could be facilitated in the presence of $Mg(AlH_4)_2$. However, the dehydrogenation mechanisms and reaction steps remain unclear. In this study, *in situ* synchrotron X-ray diffraction, which has been successfully employed to characterize the dehydrogenation behavior of $NaAlH_4$ [41] and $Mg(AlH_4)_2$ [42,12,43], is used to explore the detailed reaction steps and the synergistic effects that occur in the dehydrogenation of a $NaAlH_4$–$Mg(AlH_4)_2$ mixture.

2. Experimental

Mechano-chemical activation synthesis (MCAS) was employed to prepare magnesium aluminum hydride ($Mg(AlH_4)_2$) using sodium aluminum hydride ($NaAlH_4$, Sigma–Aldrich, 90% purity) and anhydrous magnesium chloride ($MgCl_2$,

---

* Corresponding author. Address: 1, Ta Hsueh Road, Tainan 701, Taiwan, ROC. Tel.: +886 62757575x62927; fax: +886 62754395.
E-mail address: wttsai@mail.ncku.edu.tw (W.-T. Tsai).

0925-8388/$ - see front matter © 2013 Elsevier B.V. All rights reserved.
http://dx.doi.org/10.1016/j.jallcom.2013.04.169

Sigma–Aldrich, ⩾98% purity) as precursors. By properly controlling the amount of each precursor, a mixture consisting of $Mg(AlH_4)_2$ and $NaAlH_4$ with a specific mole ratio could be fabricated according to the following reaction:

$$x\mathrm{NaAlH_4} + \mathrm{MgCl_2} \rightarrow (x-2)\mathrm{NaAlH_4} + \mathrm{Mg(AlH_4)_2} + 2\mathrm{NaCl} \quad (x = 2, 2.1, 2.5, 4, 12) \tag{1}$$

MCAS was carried out by performing ball-milling for 0.5 h in a N_2-filled vessel to avoid oxidation of the reactants and products. The details of the procedure can be found in our previous study [43].

An X-ray diffractometer (XRD, Rigaku MiniFlex II, Cu Kα radiation) was employed to identify the crystal structure of the various synthesized powders after preparation. *In situ* synchrotron X-ray diffraction (*in situ* XRD) was also performed with the aid of Synchrotron Radiation Facility (beamline 01C2 in National Synchrotron Radiation Research Center in Hsinchu, Taiwan). In each analysis, the synthesized powders were loaded in a 1-mm diameter glass capillary tube, and then mounted on the specimen holder. Flowing N_2 gas was introduced at one end of the tube, and the other end was open to the atmosphere. During the diffraction analysis, the sample was uniformly heated from room temperature to 365 °C at a heating rate of 5 °C min^{-1} by blowing hot air outside the capillary tube. The wavelength of the synchrotron X-ray was 1.033209 Å. Every 2-D diffraction pattern was successively collected by a Mar345 imaging plate. The 2-D diffraction pattern was then converted to a 1-D pattern by the Fit2D software. As a result, the high temperature transition of the crystal structure of the synthesized powders could be realized.

Thermogravimetric analysis (TGA) using a high-pressure microbalance (Cahn D-110) was employed to evaluate the dehydrogenation behavior of the synthesized powders. The amount of H_2 released and the dehydrogenation temperature were of particular interest. In each test, synthesized powders with an initial weight of ca. 500 mg were loaded in a quartz crucible and transferred into the high-pressure microbalance chamber. The chamber was evacuated to 1×10^{-4} torr followed by the introduction of H_2 gas (99.999% purity) to nearly atmospheric pressure. It was then sealed throughout the heating process. After the microbalance system was stable, the TGA test was executed from room temperature to 350 °C at a heating rate of 5 °C min^{-1}, and the results was recorded to an accuracy of ±1 µg.

3. Results and discussion

3.1. Preparation of $NaAlH_4$–$Mg(AlH_4)_2$ mixtures

X-ray diffraction analysis was performed to confirm the formation of $Mg(AlH_4)_2$ from $NaAlH_4$ and $MgCl_2$ precursors, using MCAS. The mole ratio between $NaAlH_4$ and $MgCl_2$ in the precursors varied from 2 to 12. Fig. 1 shows the XRD patterns of the as-synthesized $Mg(AlH_4)_2$ (+2 NaCl) with and without excess $NaAlH_4$. As seen in this figure, the diffraction peaks of $Mg(AlH_4)_2$ and NaCl were identified in all patterns, indicating that MCAS via reaction (1), mentioned above, was effective in preparing a sample of mixed $NaAlH_4$ and $Mg(AlH_4)_2$ powders (containing NaCl as a by-product). For the sake of convenience, the synthesized mixtures are designated as $Mg(AlH_4)_2$, 0.1 $NaAlH_4$–$Mg(AlH_4)_2$, 0.5 $NaAlH_4$–$Mg(AlH_4)_2$, and so on, with the initial precursors having mole ratios of 2, 2.1, 2.5, and so on, respectively. The diffraction peaks of $NaAlH_4$ were identified for the synthesized (0.5, 2, 10) $NaAlH_4$–$Mg(AlH_4)_2$ powders. The peak intensity of $NaAlH_4$ increased with increasing $NaAlH_4$/$Mg(AlH_4)_2$ mole ratio in the mixture. The disappearance of the $NaAlH_4$ peaks in the XRD pattern for the 0.1 $NaAlH_4$–$Mg(AlH_4)_2$ sample was due to its low concentration in the mixture.

3.2. Thermogravimetric analysis

The dehydrogenation temperatures and the corresponding amounts of H_2 released (excluding the weight of by-product NaCl) from the as-received $NaAlH_4$ and the as-synthesized $Mg(AlH_4)_2$ with the various mole ratios of $NaAlH_4$ were investigated by the thermogravimetric analysis. Fig. 2 shows the weight change of each mixture from room temperature to 350 °C (at a ramping rate of 5 °C min^{-1}) under ambient H_2 gas. As seen in this figure, the as-synthesized $Mg(AlH_4)_2$ commenced to dehydrogenate at 170 °C, while the as-received $NaAlH_4$ did so at 210 °C. The as-synthesized 0.1 $NaAlH_4$–$Mg(AlH_4)_2$ mixture showed a noticeable decrease in the initial dehydrogenation temperature to 145 °C. Furthermore, the as-synthesized (0.5, 2, 10) $NaAlH_4$–$Mg(AlH_4)_2$ mixtures exhibited not only a significant decrease in the initial dehydrogenation temperature but also a two-step weight loss characteristic as compared to both the as-synthesized $Mg(AlH_4)_2$ and the as-received $NaAlH_4$. Specifically, the initial dehydrogenation temperatures were 145 °C, 125 °C, 120 °C and 132 °C for the as-synthesized (0.1, 0.5, 2, 10) $NaAlH_4$–$Mg(AlH_4)_2$ mixtures, which were all lower than that of the as-synthesized $Mg(AlH_4)_2$ (170 °C).

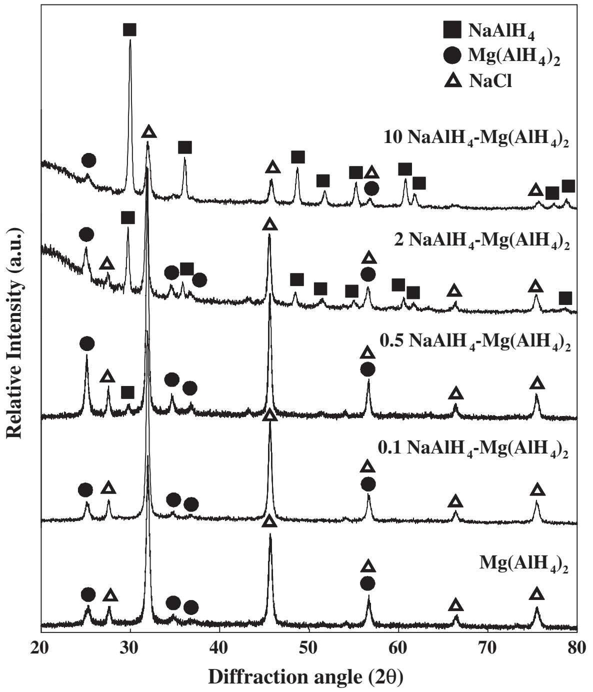

Fig. 1. XRD patterns of the as-synthesized $Mg(AlH_4)_2$ (+2 NaCl) and (0.1, 0.5, 2, 10) $NaAlH_4$–$Mg(AlH_4)_2$ (+2 NaCl) powders.

For the as-synthesized (0.5, 2, 10) $NaAlH_4$–$Mg(AlH_4)_2$ mixtures, the second dehydrogenation initiated at higher temperatures of about 184 °C, 185 °C and 195 °C, respectively. Because the initial dehydrogenation temperature of the as-synthesized $Mg(AlH_4)_2$ was lower than that of the as-received $NaAlH_4$, it is reasonable to expect that the first and the second weight loss of the as-synthesized (0.5, 2, 10) $NaAlH_4$–$Mg(AlH_4)_2$ mixtures were related to the dehydrogenation of $Mg(AlH_4)_2$ and $NaAlH_4$, respectively. The sec-

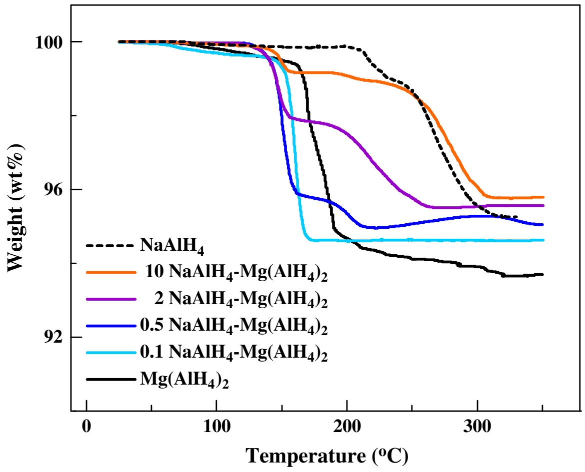

Fig. 2. Thermogravimetric analyses of the as-received $NaAlH_4$, the as-synthesized $Mg(AlH_4)_2$ (+2 NaCl) and (0.1, 0.5, 2, 10) $NaAlH_4$–$Mg(AlH_4)_2$ (+2 NaCl) powders heated from room temperature to 350 °C (ramping rate: 5 °C min^{-1}) under ambient H_2 gas.

ond dehydrogenation was therefore associated with the decomposition of $NaAlH_4$, as will be discussed later based on the results of *in situ* XRD analysis. The corresponding second dehydrogenation temperatures were also lower than that of the first dehydrogenation of the as-received $NaAlH_4$ (210 °C). The results indicate that $NaAlH_4$ and $Mg(AlH_4)_2$ are able to catalyze the dehydrogenation reactions of each other.

As shown in Fig. 2, the total amounts of H_2 released from the as-synthesized $Mg(AlH_4)_2$ (excluding the weight of NaCl) and the as-received $NaAlH_4$ for temperature up to 350 °C were 6.35 wt% and 4.80 wt%, respectively. In addition, the as-synthesized (0.1, 0.5, 2, 10) $NaAlH_4$–$Mg(AlH_4)_2$ mixtures decomposed and released 5.35 wt%, 4.95 wt%, 4.45 wt%, and 4.20 wt% H_2, respectively. Moreover, with increasing amount of $NaAlH_4$ in the mixture, more amount and higher percentage of H_2 was released from the 2nd stage dehydrogenation reaction of this compound. Specifically, 0.90 wt%, 2.40 wt%, and 3.40 wt% H_2 was released from the second dehydrogenation of the (0.5, 2, 10) $NaAlH_4$–$Mg(AlH_4)_2$ mixtures. On the basis of the original mass of the precursors used, a maximum about 69% of the theoretical amount of H_2 was thus released and measured.

3.3. In situ synchrotron XRD analysis

Srivastava et al. [40] presented the synergistic benefits of $Mg(AlH_4)_2$ on lowering the dehydrogenation temperature and accelerating the H_2 desorption rate of $NaAlH_4$. Our previous study [43] reported the effect of the minor and residual $NaAlH_4$ on facilitating the decomposition of $Mg(AlH_4)_2$ and lowering the temperature needed for the first step dehydrogenation temperature. However, the detailed mechanisms underlying the synergistic effects between $NaAlH_4$ and $Mg(AlH_4)_2$ are still unclear. Therefore, *in situ* synchrotron X-ray diffraction (*in situ* synchrotron XRD) technique was applied to characterize the dehydrogenation reactions and mechanisms involved.

During *in situ* synchrotron X-ray diffraction analysis, the powders were heated at a rate of 5 °C min^{-1} from room temperature up to 365 °C to induce the dehydrogenation reactions. The diffraction patterns were then collected and compiled every 20 °C. Fig. 3 shows the *in situ* synchrotron XRD patterns of the 0.1 $NaAlH_4$–$Mg(AlH_4)_2$ powder mixture heated from room temperature to 365 °C. As shown in this figure, $Mg(AlH_4)_2$ and NaCl were stable, and no significant phase transformation was observed below 125 °C. However, when increasing the temperature to 145 °C, the MgH_2 and Al peaks appeared, while the intensity of $Mg(AlH_4)_2$ peaks decreased, indicating the occurrence of the first step dehydrogenation reaction:

$$Mg(AlH_4)_2 \rightarrow MgH_2 + 2Al + 3H_2 \tag{2}$$

The temperature-dependent X-ray diffraction peak intensity, derived from Fig. 3a, is summarized in Fig. 3b. The results clearly show that the initial decomposition occurred at a temperature between 125 and 145 °C, consistent with that measured by TGA results shown in Fig. 2. The initial dehydrogenation temperature of $Mg(AlH_4)_2$ was significantly lowered because of the presence of $NaAlH_4$. The catalytic effect of $NaAlH_4$ on lowering the initial dehydrogenation temperature of $Mg(AlH_4)_2$ was confirmed by *in situ* XRD analysis. The Mg_2Al_3 peaks, along with the gradually decreasing intensity of the MgH_2 and Al peaks, were observed as the temperature was increased to 305 °C, indicating the occurrence of the second step dehydrogenation associated with the following reaction:

$$2MgH_2 + 3Al \rightarrow Mg_2Al_3 + 2H_2 \tag{3}$$

Nevertheless, the TGA results shown in Fig. 2 indicate that less H_2 was released in the second step dehydrogenation than in the first. The dehydrogenation reactions (2) and (3) were the same as those of the as-synthesized $Mg(AlH_4)_2$ (shown in our previous study [43]), although the initial dehydrogenation temperature changed with the presence of $NaAlH_4$. In the 0.1 $NaAlH_4$–$Mg(AlH_4)_2$ powder mixture, the decomposition reaction of $NaAlH_4$ at low concentration was not significantly affected by the presence of $Mg(AlH_4)_2$.

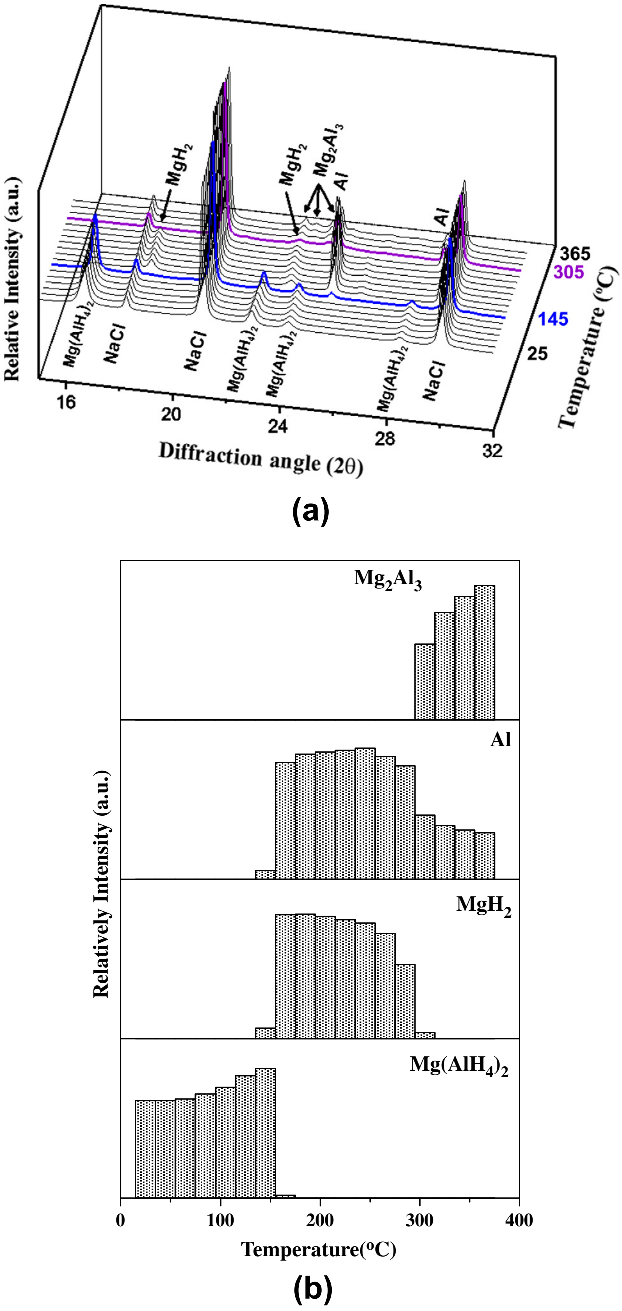

Fig. 3. (a) *In situ* synchrotron XRD patterns of the 0.1 $NaAlH_4$–$Mg(AlH_4)_2$ (+2 NaCl) heated from room temperature to 365 °C and (b) variation of the strongest peak intensity with temperature for the major species appeared during thermal dehydrogenation.

Fig. 4a shows the *in situ* synchrotron XRD patterns of the 0.5 $NaAlH_4$–$Mg(AlH_4)_2$ powder mixture heated from room temperature to 365 °C. As seen in this figure, $NaAlH_4$ and $Mg(AlH_4)_2$ were stable at temperatures lower than 125 °C. As the temperature increased to 145 °C, the MgH_2 and Al peaks indicated the commencement of the first step dehydrogenation reaction of $Mg(AlH_4)_2$ in accordance with reaction (2). The temperature-dependent diffraction peak intensity shown in Fig. 4b indicates that the decomposition of $NaAlH_4$ took place according to the following reaction:

$$3NaAlH_4 \rightarrow Na_3AlH_6 + 2Al + 3H_2 \quad (4)$$

This reaction started to occur at 185 °C, which was lower than that of pure $NaAlH_4$. This result suggests that MgH_2 and/or Al, the products of the first step dehydrogenation reaction of $Mg(AlH_4)_2$, play a catalytic role in lowering the initial dehydrogenation temperature of $NaAlH_4$. This finding is in good agreement with the TGA results shown in Fig. 2.

The diminishing intensity of Na_3AlH_6 peaks from 285 to 325 °C might be associated with the following third step dehydrogenation reaction of the mixture:

$$2Na_3AlH_6 \rightarrow 6NaH + 2Al + 3H_2 \quad (5)$$

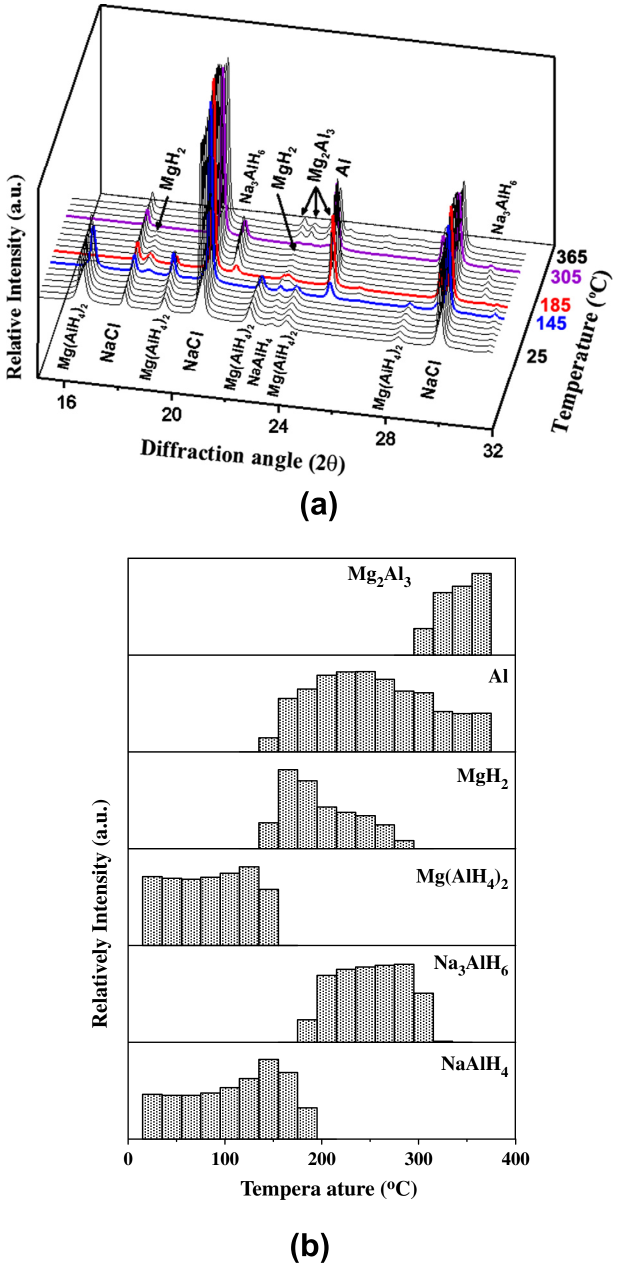

Fig. 4. (a) *In situ* synchrotron XRD patterns of the 0.5 $NaAlH_4$–$Mg(AlH_4)_2$ (+2 NaCl) heated from room temperature to 365 °C and (b) variation of the strongest peak intensity with temperature for the major species appeared during thermal dehydrogenation.

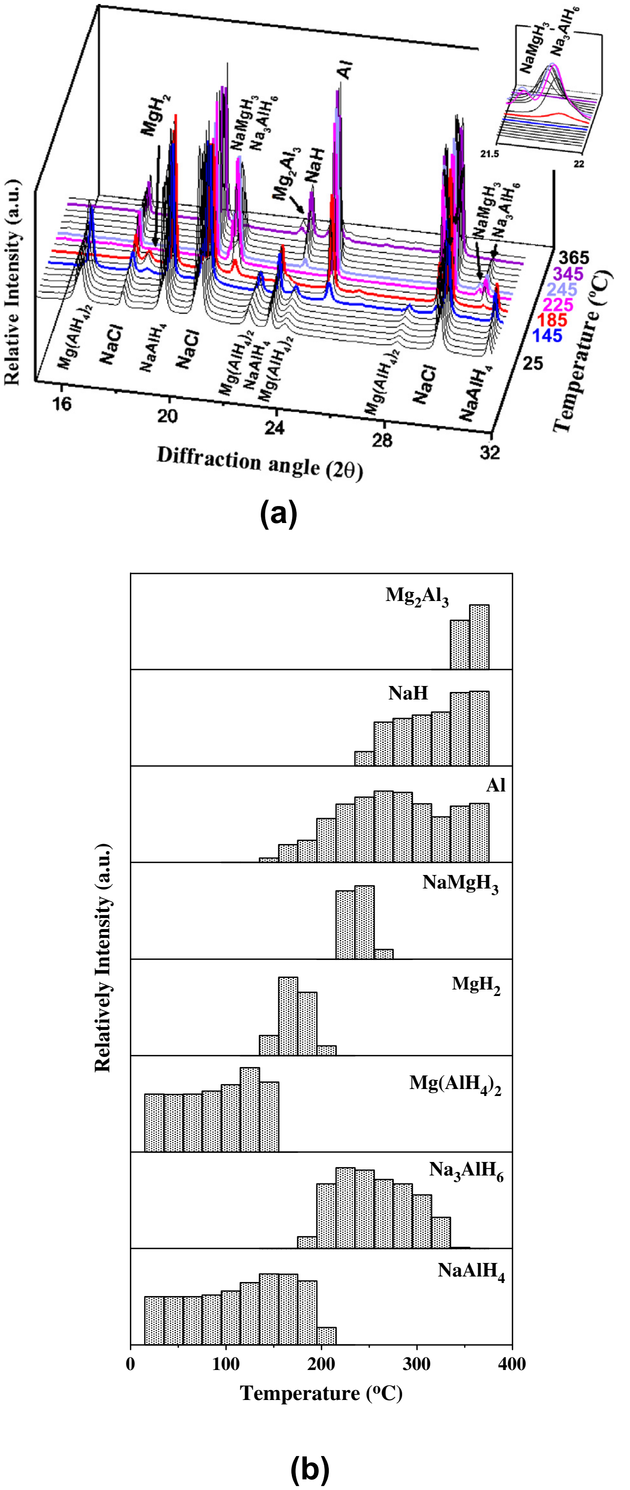

Fig. 5. (a) *In situ* synchrotron XRD patterns of the 2 $NaAlH_4$–$Mg(AlH_4)_2$ (+2 NaCl) heated from room temperature to 365 °C and (b) variation of the strongest peak intensity with temperature for the major species appeared during thermal dehydrogenation.

This phenomenon was more pronounced for $NaAlH_4$-rich mixtures, as will be discussed later. As the 0.5 $NaAlH_4$–$Mg(AlH_4)_2$ powder mixture continued to heat up to 305 °C, the fourth step dehydrogenation reaction accompanied by the formation of Mg_2Al_3 via reaction (3) was found.

Fig. 5a shows the *in situ* synchrotron XRD patterns of the 2 $NaAlH_4$–$Mg(AlH_4)_2$ powder mixture heated from room temperature to 365 °C. Basically, the results were similar to those for the 0.5 $NaAlH_4$–$Mg(AlH_4)_2$ powders at temperatures below 185 °C. Nonetheless, Fig. 5b shows a noticeable $NaMgH_3$ peak at temperatures above 225 °C, according to the following reaction:

$$2Na_3AlH_6 + 6MgH_2 \rightarrow 6NaMgH_3 + 2Al + 3H_2 \quad (6)$$

Previous studies [39,44–46] reported that $NaMgH_3$ forms as the result of reacting $NaAlH_4$ with MgH_2. However, since $NaAlH_4$ was absent at 225 °C, as revealed in Fig. 5b, reaction (6) was more likely responsible for the formation of $NaMgH_3$. Fig. 5b shows that NaH appeared at the expense of Na_3AlH_6 above 245 °C via reaction (5). The formation of Mg_2Al_3 via reaction (3) was again identified above 345 °C. Moreover, the following reaction:

$$2NaMgH_3 + 3Al \rightarrow Mg_2Al_3 + 2NaH + 2H_2 \quad (7)$$

also contributed to the formation of the intermetallic compound. The results shown in Figs. 4 and 5 indicated that the mole ratio between $NaAlH_4$ and $Mg(AlH_4)_2$ can greatly affect the dehydrogenation behavior of each compound. $NaAlH_4$ in the mixture caused a decrease of the initial dehydrogenation temperature of $Mg(AlH_4)_2$, while the dehydrogenated products of $Mg(AlH_4)_2$, specifically MgH_2 and/or Al, facilitated the dehydrogenation of $NaAlH_4$ towards a lower temperature. With increasing amount of $Mg(AlH_4)_2$, the decrease of the dehydrogenation temperature of $NaAlH_4$ became more significant. Besides, the composition of the powder mixtures can also contribute to a notable difference in the formation of the intermediate reaction products during heating as described in reactions (6) and (7).

4. Conclusions

The mixture of $NaAlH_4$ and $Mg(AlH_4)_2$ exhibited multiple-step dehydrogenation processes during heating from room temperature to 350 °C, with at least five steps being identified. The first step dehydrogenation was attributed to the decomposition of $Mg(AlH_4)_2$, while the second step was mainly associated with $NaAlH_4$. A maximum about 69% of the theoretical H_2 was released from the mixture with a $NaAlH_4$:$Mg(AlH_4)_2$ mole ratio of 10:1. Each complex metal hydride acted as a catalyst in lowering the initial dehydrogenation temperature of the other in the mixture. The initial dehydrogenation reaction temperature for $Mg(AlH_4)_2$ was lowered from 170 °C to 120 °C with the presence of $NaAlH_4$, while that of the latter decreased from 210 °C to 184 °C. The mutual catalytic roles of $NaAlH_4$ and $Mg(AlH_4)_2$ in the mixture were confirmed by TGA and *in situ* synchrotron XRD analyses.

Acknowledgements

The authors gratefully acknowledge the financial support from the National Science Council of the Republic of China (Taiwan) under Grant NSC 100-2221-E-006-245-MY2 and the Research Center for Energy Technology and Strategy, National Cheng Kung University under Grant D100-23003.

References

[1] D. Chandra, J.J. Reilly, R. Chellappa, JOM 58 (2006) 26–32.
[2] S. Orimo, Y. Nakamori, J.R. Eliseo, A. Zuttel, C.M. Jensen, Chem. Rev. 107 (2007) 4111–4132.
[3] B. Sakintuna, F. Lamari-Darkrim, M. Hirscher, Int. J. Hydrogen Energy 32 (2007) 1121–1140.
[4] Y. Nakamori, H.W. Li, M. Matsuo, K. Miwa, S. Towata, S. Orimo, J. Phys. Chem. Solids 69 (2008) 2292–2296.
[5] E. Wiberg, R. Bauer, Z. Naturforsch 5b (1950) 396–397.
[6] M. Fichtner, O. Fuhr, J. Alloys Comp. 345 (2002) 286–296.
[7] M. Fichtner, J. Engel, O. Fuhr, A. Gloss, O. Rubner, R. Ahlrichs, Inorg. Chem. 42 (2003) 7060–7066.
[8] K. Komiya, N. Morisaku, Y. Shinzato, K. Ikeda, S. Orimo, Y. Ohki, K. Tatsumi, H. Yukawa, M. Morinaga, J. Alloys Comp. 446–447 (2007) 237–241.
[9] R.A. Varin, Ch. Chiu, T. Czujko, Z. Wronski, Nanotechnology 16 (2005) 2261–2274.
[10] R.A. Varin, Ch. Chiu, T. Czujko, Z. Wronski, J. Alloys Comp. 439 (2007) 302–311.
[11] M. Mamatha, B. Bogdanovic, M. Felderhoff, A. Pommerin, W. Schmidt, F. Schüth, C. Weidenthaler, J. Alloys Comp. 407 (2006) 78–86.
[12] M. Mamatha, C. Weidenthaler, A. Pommerin, M. Felderhoff, F. Schüth, J. Alloys Comp. 416 (2006) 303–314.
[13] Y. Kim, E.K. Lee, J.H. Shim, Y.W. Cho, K.B. Yoon, J. Alloys Comp. 422 (2006) 283–287.
[14] B. Bogdanovic, M. Schwickardi, J. Alloys Comp. 253–254 (1997) 1–9.
[15] P.A. Berseth, A.G. Harter, R. Zidan, A. Blomqvist, C.M. Araujo, R.H. Scheicher, R. Ahuja, P. Jena, Nano Lett. 9 (2009) 1501–1505.
[16] C. Wu, H.M. Cheng, J. Mater. Chem. 20 (2010) 5390–5400.
[17] F. Schüth, B. Bogdanović, A. Taguchi (inventors), MPI Mühlheim, Germany, assignee, Materials encapsulated in porous matrices for the reversible storage of hydrogen, Patent application WO 2005014469, 2003.
[18] A. Gutowska, L. Li, Y. Shin, C.M. Wang, X.S. Li, J.C. Linehan, R.S. Smith, B.D. Kay, B. Schmid, W. Shaw, M. Gutowski, T. Autrey, Angew. Chem. Int. Ed. 44 (2005) 3578–3582.
[19] C.P. Baldé, B.P.C. Hereijgers, J.H. Bitter, K.P. de Jong, Angew. Chem. Int. Ed. 45 (2006) 3501–3503.
[20] C.P. Baldé, B.P.C. Hereijgers, J.H. Bitter, K.P. de Jong, J. Am. Chem. Soc. 130 (2008) 6761–6765.
[21] P.E. de Jongh, P. Adelhelm, ChemSusChem 3 (2010) 1332–1348.
[22] T.K. Nielsen, F. Besenbacher, T.R. Jensen, Nanoscale 3 (2011) 2086–2098.
[23] J.J. Vajo, Curr. Opin. Solid State Mater. Sci. 15 (2011) 52–61.
[24] J.J. Vajo, G.L. Olson, Scr. Mater. 56 (2007) 829–834.
[25] S.V. Alapati, J.K. Johnson, D.S. Sholl, Phys. Chem. Chem. Phys. 9 (2007) 1438–1452.
[26] C. Wolverton, D.J. Siegel, A.R. Akbarzadeh, V. Ozoliņš, J. Phys.: Condens. Matter 20 (2008) 064228.
[27] J.J. Vajo, F. Mertens, C.C. Ahn, R.C. Bowman, B. Fultz, J. Phys. Chem. B 108 (2004) 13977–13983.
[28] J.J. Vajo, S.L. Skeith, F. Mertens, J. Phys. Chem. B 109 (2005) 3719–3722.
[29] U. Bösenberg, S. Doppiu, L. Mosegaard, G. Barkhordarian, N. Eigen, A. Borgschulte, T.R. Jensen, Y. Cerenius, O. Gutfleisch, T. Klassen, M. Dornheim, R. Bormann, Acta Mater. 55 (2007) 3951–3958.
[30] K. Crosby, L.L. Shaw, Int. J. Hydrogen Energy 35 (2010) 7519–7529.
[31] P.J. Wang, Z.Z. Fang, L.P. Ma, X.D. Kang, P. Wang, Int. J. Hydrogen Energy 33 (2008) 5611–5616.
[32] P. Sridechprasat, Y. Suttisawat, P. Rangsunvigit, B. Kitiyanan, S. Kulprathipanja, Int. J. Hydrogen Energy 36 (2011) 1200–1205.
[33] M.Q. Fan, L.X. Sun, Y. Zhang, F. Xu, J. Zhang, H.L. Chu, Int. J. Hydrogen Energy 33 (2008) 74–80.
[34] Y. Zhang, Q.F. Tian, S.S. Liu, L.X. Sun, J. Power Sources 185 (2008) 1514–1518.
[35] A.W. Vittetoe, M.U. Niemann, S.S. Srinivasan, K. McGrath, A. Kumar, D.Y. Goswami, E.K. Stefanakos, S. Thomas, Int. J. Hydrogen Energy 34 (2009) 2333–2339.
[36] R. Chen, X. Wang, L. Xu, L. Chen, S. Li, C. Chen, Mater. Chem. Phys. 124 (2010) 83–87.
[37] J. Mao, Z. Guo, X. Yu, M. Ismail, H. Liu, Int. J. Hydrogen Energy 36 (2011) 5369–5374.
[38] R.A. Varin, T. Czujko, C. Chiu, R. Pulz, Z.S. Wronski, J. Alloys Comp. 483 (2009) 252–255.
[39] M. Ismail, Y. Zhao, X.B. Yu, J.F. Mao, S.X. Dou, Int. J. Hydrogen Energy 36 (2011) 9045–9050.
[40] M.S.L. Hudson, D. Pukazhselvan, G.I. Sheeja, O.N. Srivastava, Int. J. Hydrogen Energy 32 (2007) 4933–4938.
[41] K.J. Gross, S. Guthrie, S. Takara, G. Thomas, J. Alloys Comp. 297 (2000) 270–281.
[42] A. Fossdal, H.W. Brinks, M. Fichtner, B.C. Hauback, J. Alloy. Compd. 404–406 (2005) 752–756.
[43] C.H. Yang, T.T. Chen, W.T. Tsai, J. Alloys Comp. 525 (2012) 126–132.
[44] P.A. Berseth, J. Pittman, K. Shanahan, A.C. Stowe, D. Anton, R. Zidan, J. Phys. Chem. Solids 69 (2008) 2141–2145.
[45] S. Sartori, X. Qi, N. Eigen, J. Muller, T. Klassen, M. Dornheim, B.C. Hauback, Int. J. Hydrogen Energy 34 (2009) 4582–4586.
[46] X. Rafi-ud-din, P. Qu, L. Li, M. Zhang, M.Z. Ahmad, M.Y. Iqbal, M.H. Rafique, RSC Adv. 2 (2012) 4891–4903.